Mineralogical Magazine, February 1999, Vol. 63(1), pp. 17–26

The structure of antimonian dussertite and the role of antimony in oxysalt minerals

U. Kolitsch[1], P. G. Slade[2], E. R. T. Tiekink[3] and A. Pring[1]

[1] Department of Mineralogy, South Australian Museum, North Terrace, Adelaide, S. A. 5000, Australia
[2] CSIRO Land and Water, Private Bag No. 2, Glen Osmond, S. A. 5064, Australia
[3] Department of Chemistry, The University of Adelaide, Australia 5005

ABSTRACT

The structure of antimonian dussertite, $Ba(Fe^{3+}_{0.84},Sb^{5+}_{0.16})_3(AsO_4)_2(OH,H_2O)_6$, has been refined in space group $R\bar{3}m$ with a 7.410(3), c 17.484(4) Å, $Z = 3$, to $R = 3.2$ % and $R_w = 3.7$ % using 377 observed reflections with $I \geqslant 3\ \sigma(I)$. The structure is of the alunite-type and consists of sheets of corner-sharing $(Fe^{3+},Sb^{5+})O_6$ octahedra parallel to (0001). The substitution of Sb^{5+} for Fe^{3+}, and not for As^{5+}, is unambiguously demonstrated not only by the structure refinement but also by electron microprobe analyses and crystal-chemical considerations. The icosahedrally coordinated Ba cations occupy cavities between pairs of octahedral sheets and are surrounded by six O atoms from the AsO_4 tetrahedra and six O atoms from the $(Fe^{3+},Sb^{5+})O_6$ octahedra. The mean bond lengths for the various coordination polyhedra are As-O 1.684(3) Å, (Fe,Sb)-O 2.004(1) Å, and Ba-O 2.872(2) Å. A hydrogen-bonding network is modelled using bond-valence calculations. The dussertite sample investigated is the first member of the crandallite group found to contain substantial Sb.

Keywords: dussertite, crystal structure, crystal chemistry, antimony, crandallite group.

Introduction

As part of a project designed to examine the feasibility of using certain mineral structure types as hosts for the safe and long-term immobilisation of toxic heavy metals such as Pb, Tl, Hg, As, Sb and Cr, an evaluation of members of the crandallite (phosphate), beudantite (arsenate-sulphate, phosphate-sulphate) and alunite (sulphate) mineral groups has been undertaken. In this context the crystal chemistry and crystallography of these mineral groups is of major interest. Kolitsch and Pring (to be published) have shown that members of these mineral groups can be used, under certain conditions, as stable and reliable hosts for toxic heavy metals.

The present study focuses on the crystal structure and crystal chemistry of antimonian dussertite from the Clara baryte and fluorite mine, Black Forest, Germany. Dussertite, $BaFe_3(AsO_4)_2(OH,H_2O)_6$, a rare member of the crandallite group, was originally described from Djebel Debar, Constantine, Algeria, where it occurs as minute green crystals flattened {0001} and grouped as rosettes or as crusts (Palache *et al.*, 1951). Dussertite belongs to a large family of isostructural compounds with the general formula $AB_3(XO_4)_2(OH,H_2O)_6$, where A = monovalent (H_3O, Na, K, Ag, Tl, ...), divalent (Ca, Sr, Ba, Pb, Hg, ...), trivalent (Bi, *REE*) or a quadrivalent cation (Th, Zr), B = trivalent cation (Al, Fe, Cr, ; and minor Cu^{2+}, Zn^{2+}, Nb^{5+}, Ta^{5+}) and X = P^{5+}, As^{5+}, S^{6+}, Cr^{6+} and minor Si (Palache *et al.*, 1951; Lottermoser, 1990; Schwab *et al.*, 1990; Lengauer *et al.*, 1994; Fleischer and Mandarino, 1995, 1997). Solid solution among these compounds is extensive (e.g. Wise, 1975; Scott, 1987; de Bruiyn *et al.*, 1990; Rattray *et al.*, 1996; Birch and van der Heyden, 1997) and no conclusive evidence for miscibility gaps has yet been found.

The space group of these predominantly rhombohedral compounds is generally $R\bar{3}m$; however, other symmetries are known: gorceixite, $BaAl_3(PO_4)_2(OH,H_2O)_6$, shows very slight departures from rhombohedral symmetry and crystallises in space group *Cm* (Radoslovich and Slade, 1980; Radoslovich, 1982; Blanchard, 1989); an apparent triclinic dimorph of crandallite, $CaAl_3(PO_4)_2(OH,H_2O)_6$, was reported by Cowgill *et al.* (1963), a specific crystal of beudantite, $PbFe_3(AsO_4)(SO_4)(OH,H_2O)_6$, was shown by Szymański (1988) to have obvious triclinic symmetry; and a strongly pseudohexagonal orthorhombic jarosite was noted by Jambor and Dutrizac (1983).

For crandallite and, most probably, for woodhouseite, Kato and Radoslovich (1968), Blount (1974) and Kato (1977) found that the divalent Ca ions are disordered around their sites. Similar disorder for Pb has also been detected in plumbojarosite (Szymański, 1985), beudantite (Szymański, 1988; Giuseppetti and Tadini, 1989) and kintoreite (Kharisun *et al.*, 1997).

Ordering on the XO_4 site has been a matter of some debate. Structure determinations of beudantite, $PbFe_3(AsO_4,SO_4)(OH,H_2O)_6$ (Szymański, 1988; Giuseppetti and Tadini, 1989), and of an arsenatian sulphatian kintoreite, $PbFe_3(PO_4,AsO_4,SO_4)(OH,H_2O)_6$ (Kharisun *et al.*, 1997), showed that the XO_4 anions are disordered and that the space group is $R\bar{3}m$. This is at variance with the results of Giuseppetti and Tadini (1987) who reported that PO_4^{3-} and SO_4^{2-} in corkite, $PbFe_3(PO_4)(SO_4)(OH,H_2O)_6$, are ordered and thus the space group is $R3m$. A corresponding ordering scheme for AsO_4^{3-} and SO_4^{2} was observed in gallobeudantite (Jambor *et al.*, 1996).

A large number of the crandallite and beudantite group minerals show anomalous optical behaviour such as biaxial optics (with 2V usually between 0 and 20° but in some cases up to 70°) or biaxial regions in otherwise uniaxial crystals, sector growth, twinning and anomalous interference colours (e.g. Hintze, 1933; Palache *et al.*, 1951; Walenta, 1966; Szymański, 1985). No serious effort has been made so far to explain these anomalies which may indicate that some crystals are not perfectly rhombohedral.

The metal and semi-metal cations in the dussertite structure, Ba, Fe and As, are the largest cations that have been observed as major constituents in natural members of the alunite family of compounds. The crystallography and crystal chemistry of dussertite was therefore of special interest. The present contribution describes the previously unknown crystal structure of an antimonian dussertite and discusses the role of Sb in oxysalt minerals.

Experimental

The dussertite specimen from which the crystals used in this study came was from the Clara mine, Germany. The specimen consists of unusually sharp, single crystals up to 0.3 mm, scattered on a goethite-covered matrix of corroded baryte. The yellowish to olive-green, transparent crystals are consistently composed of lustrous positive $\{10\bar{1}2\}$ and negative $\{01\bar{1}2\}$ rhombohedra of almost equal size, with the top of each crystal capped by a small, triangular basal face {0001} of matt appearance. The dussertite apparently was formed by the interaction of arsenate- and iron-rich solutions with the baryte gangue. A similar genesis has been reported for the Al analoue of dussertite, arsenogorceixite ($BaAl_3(AsO_4)_2(OH,H_2O)_6$; Walenta, 1966).

A preliminary investigation of the chemical composition of several crystals from the sample was done by energy-dispersive X-ray spectroscopy (EDS) in a scanning electron microscope (SEM). The analyses showed the crystals to contain significant amounts of Sb. For quantitative analysis by wavelength-dispersive X-ray spectroscopy, a Cameca 'Camebax 51' electron microprobe was used. These measurements, conducted on polished and carbon-coated crystals, were supplemented by qualitative EDS. The crystals proved to be stable under the electron beam as shown by the use of different beam diameters. Besides the major cations Ba, Fe and As, a considerable amount of Sb was confirmed, but the absolute Sb content was slightly variable. The Fe/Sb ratio was 5.4 (average of 6 analyses, range: 2.8–6.5). Contrast-enhanced backscattered electron images were unable to distinguish any chemical inhomogeneities. The following elements were detected in very small to trace amounts (in order of decreasing abundance): Sr, F, Al, Si, P, Cu, Si, K, Ca. Elements searched for but not detected were Pb, Ce and Bi. An idealised empirical formula $Ba_{0.9}(Fe^{3+}_{0.84},Sb^{5+}_{0.16})_{2.6}(AsO_4)_2(OH,H_2O)_6$ was calculated on the basis of 2 XO_4, as recommended by Scott (1987). Vacancies were assumed not to be present. The assignment of Sb to the Fe site was supported by the results of the structure refinement (see below).

To investigate any possible deviation from uniaxial behaviour, the optical properties were carefully determined on grain mounts in white light, using Cargille immersion liquids. The grains were found to be uniaxial negative, slightly pleochroic, O greenish yellow, E pale yellow to colourless, ε 1.840 $\pm$ 0.005, ω 1.865 $\pm$ 0.005. The refractive indices are close to those reported previously (1.85, 1.87, Barth and Berman, 1930; 1.845, 1.870, Foshag, 1937; ~1.87 with rather low birefringence, Walenta, 1966). The dussertite crystals investigated by Foshag (1937) were reported to be uniaxial to abnormally biaxial with $2V = 15-20$. No such biaxial optics were noticed in the present study. However, slightly anomalous, bluish-grey to bluish interference colours were observed throughout. Unlike the dussertite of Walenta (1966), for some of which a more or less pronounced sector growth was reported, no such anomaly was observed during the present study. Rarely, some crystal fragments exhibit very faint striation growth features parallel to the crystal faces. No evidence of twinning was found. For comparison, and to evaluate possible effects of the high Sb content, an olive-green dussertite specimen from the type locality in Algeria was also investigated optically. It is uniaxial negative (or biaxial with a very small optical angle) and shows the same anomalous bluish interference colours. A semiquantitative analysis revealed only Ba, Fe and As, along with traces of Cu, and confirmed this specimen to have an almost end-member composition. Therefore, the presence of Sb does not influence the optical properties in an obvious way.

Several single crystals were removed from the sample and, after being checked with a polarising microscope, two were selected for investigation by Weissenberg and precession methods. The diffraction patterns did not reveal any deviation from rhombohedral symmetry and enabled the space group to be determined as $R32$, $R3m$ or $R\bar{3}m$. The crystal showing the sharpest reflections was mounted on a Rigaku AFC6R rotating anode four-circle single-crystal diffractometer. Unit cell dimensions, refined from 11 reflections ($2\theta = 53.9-54.8^\circ$), are $a = 7.410(3)$ and $c = 17.484(4)$ Å. Intensity data were measured at room temperature using graphite monochromatised Mo-$K\alpha$ radiation and the ω-2θ scan technique for a full sphere of reciprocal space such that $\theta_{max} =$ 32.5 (Table 1). A total of 2157 reflections representing 409 unique reflections were measured, out of which 32 with $I < 3\sigma(I)$ were considered unobserved and excluded from the refinement. The data were corrected for Lorentz and polarisation effects, for anomalous dispersion, and an analytical absorption correction, based on the crystal size and faces, was applied (de Meulenaer and Tompa, 1965). Normalised structure-factor statistics clearly indicated the centrosymmetric space group $R\bar{3}m$. As input values for the atomic positions of Ba, Fe, As and O, the data reported for kintoreite (Kharisun *et al.*, 1997) were used. Scattering factors for neutral atoms were taken from the International Tables for X-ray Crystallography (1974). After the refinement of the scale factor and positional and isotropic displacement parameters, R was 7.3 %, and a large, positive residual electron density remained on the Fe site but not on the As site. Therefore, and on account of crystal-chemical considerations (see discussion), Sb was allocated to the Fe site. After introducing anisotropic displacement parameters for Ba, (Fe,Sb) and As, and constraining the displacement parameters for Sb and Fe, the intensity data were merged and R dropped to 3.8 %. The displacement parameters were then held constant and the individual occupancies of Fe and Sb on their common site were adjusted. A further drop of R to 3.3 % resulted and the Fe/Sb ratio obtained was 0.84(2)/0.16(2). At convergence, R = 3.2 % and R_W = 3.7 %. The final electron density map was relatively flat, with the maximum value (1.3 e/Å^3) near the position of O(3). Hydrogen atoms could not be located unambiguously. All computations were carried out with version 1.6 of the teXsan suite of computer programs (Molecular Structure Corporation, 1993). Bond-valence calculations using the program EUTAX (O'Keeffe, 1991; Brese and O'Keeffe, 1991) helped to model the hydrogen-bonding network and establish the crystal-chemical reliability of the structure refinement.

Results and discussion

The final atomic coordinates and displacement parameters for the structure are listed in Table 2, and selected interatomic distances and bond angles are given in Table 3. A summary of the bond-valence calculations for the structure is provided in Table 4, and a full list of observed and calculated structure factors for the final refinement are given in Table 5 (deposited with the Editor).

The crystal structure of dussertite is similar to that of crandallite (Blount, 1974) and closely related to the structures of the beudantite and alunite groups. The individual metal-oxygen polyhedra are shown in Figs. 1–3.

Calculated bond-valence sums (BVSs) suggest that both O(1) and O(3) are bonded to hydrogens, at least partly (Table 4). In other crandallite-type

TABLE 1. Crystal data, data collection information and refinement details for antimonian dussertite

Crystal data:	
Formula	$Ba(Fe_{0.84},Sb_{0.16})_3(AsO_4)_2(OH,H_2O)_6$
Formula weight	716.43
Crystal system	Rhombohedral
Space group	$R\bar{3}m$
a, c (Å)	7.410(3), 17.484(4)
V (Å^3), Z	831.3(3), 3
D(calc.) (g/cm^3)	4.293
$F(000)$	990
μ (cm^{-1})	138.9
Absorption correction	analytical
Transmission factors	0.093–0.246
Crystal dimensions (mm)	0.16 × 0.16 × 0.16
Data Collection:	
Diffractometer	Rigaku AFC6R (rotating anode)
Scan mode	ω-2θ
Temperature (K)	293
λ (Mo-$K\alpha$) (Å)	0.71073
θ range (°)	3–32.5
h, k, l ranges	$-11 \rightarrow 11$, $-11 \rightarrow 11$, $-26 \rightarrow 26$
Total reflections measured	2157
Unique reflections	409
Refinement:	
Refinement on	F
Weighting scheme	$1/[\sigma^2(F_0) + (0.019F_0)^2]$
R, R_W	3.2 %, 3.7 %
Refls. used in refinement	377 ($I \geqslant 3\sigma(I)$)
No. of refinable parameters	18
$(\Delta/\sigma)_{max}$	0.0022
$\Delta\rho_{min}$, $\Delta\rho_{max}$ (e/Å^3)	−1.1, 1.3

TABLE 2. Fractional atomic coordinates and displacement parameters for antimonian dussertite (s.u.s in parentheses)

Atom	x	y	z	U_{eq}	Occupancy
Ba	0.0	0.0	0.0	0.0155(1)	
Fe	0.5	0.0	0.5	0.0136(1)	0.84(2)
Sb	0.5	0.0	0.5	0.0136(1)	0.16(2)
As	0.0	0.0	0.31047(7)	0.0127(1)	
O(1)	0.0	0.0	0.5929(5)	0.018(2)	
O(2)	0.2099(4)	−x	−0.0554(3)	0.0145(8)	
O(3)	0.1260(4)	−x	0.1366(2)	0.0131(8)	

	U_{11}	U_{22}	U_{33}	U_{12}	U_{13}	U_{23}
Ba	0.0148(3)	U_{11}	0.0171(4)	$0.5U_{11}$	0.0	0.0
Fe/Sb	0.0124(4)	0.0094(7)	0.0184(5)	$0.5U_{22}$	0.0003(2)	$2U_{13}$
As	0.0101(3)	U_{11}	0.0179(5)	$0.5U_{11}$	0.0	0.0

TABLE 3. Interatomic distances (Å) and bond angles (°) for the coordination polyhedra in antimonian dussertite

Ba-O(2)	2.863(5) × 6	(Fe,Sb)-O(2)	2.023(4) × 2	As-O(1)	1.689(9)
Ba-O(3)	2.885(6) × 6	(Fe,Sb)-O(3)	2.002(2) × 4	As-O(2)	1.683(5) × 3

XO_6 octahedron X = (Fe,Sb)		AsO$_4$ tetrahedron	
O(2) - X - O(3)	86.0(2) × 4	O(1) - As - O(2)	109.8(2) × 3
O(2) - X - O(3)	94.0(2) × 4	O(2) - As - O(2)	109.2(2) × 3
O(3) - X - O(3)	88.8(3) × 2		
O(3) - X - O(3)	91.2(3) × 2		
O(3) - X - O(3)	180(-) × 2		
O(2) - X - O(2)	180(-)		

structures, O(3) is generally considered to be a hydroxyl and O(1) half of a hydroxyl (e.g. crandallite, kintoreite). Thus, hydrogen bonds can be postulated for only three of the six O(1)-O(3) contacts (contact lengths 3 × 2.88 Å), but not for the O(1)-O(1) contacts (3.25 Å), the O(1)-O(2) contact (2.76 Å), or for two of the four O(2)-O(3) contacts (2 × 2.74 Å). These hydrogen bonds must be both weak and bent since the O(1)-O(3) bond distances are large compared to the average distance O···O of the hydrogen bond in monoprotonated arsenate groups (2.61 Å, Ferraris and Ivaldi, 1984).

If O(3) is a donor, the BVSs calculated with the inclusion of the estimated hydrogen-bonding contributions according to Brown and Altermatt (1985) would give ~2.10 *vu* (valence units) and ~1.39 *vu* for O(3) and O(1), respectively. This would agree with the observation that about half of the O(1) atoms are protonated. Stereochemical considerations also suggest O(3) represents the donor, as it is the only O coordinated to Ba and (Fe,Sb) but not As, and the Fe-O(3) distances are slightly shorter than the Fe-O(2) distances (2.002(2) *vs* 2.023(2) Å). If O(1) were a donor, it would represent the hydroxyl in a monoprotonated arsenate group and the As-O(H) distance would be expected to be smaller than the three other As-O distances (Ferraris and Ivaldi, 1984). This is clearly not the case (Table 3). Nonetheless, our data are not sufficient to exclude any positional disorder of the hydrogen.

TABLE 4. Results of empirical bond-valence calculations for antimonian dussertite

	Ba	Fe,Sb	As	Sum
O(1)			1.23	1.23# (~1.39)*
O(2)	0.21 (× 6)	0.54 (× 2)	1.25 (× 3)	2.00#
O(3)	0.20 (× 6)	0.57 × 2 (× 4)		1.34# (~2.10)*
Sum	2.46	3.36#	4.98	

The sum values for O(1,2,3) and (Fe,Sb) correspond to the refined occupancy of the (Fe,Sb) site. Calculations for Fe^{3+} alone gave 3.05 *vu* and for Sb^{5+} alone 5.01 *vu*. The sum value of 3.36 *vu* reflects the increased average valency.

* Values in parentheses are obtained after adding the H bond contributions (see text).

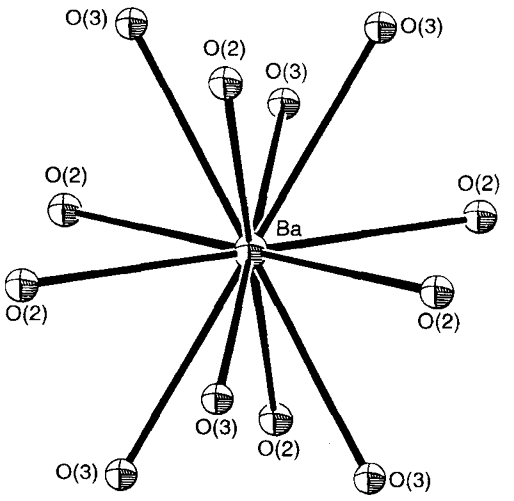

FIG. 1. The unusually regular, icosahedral BaO$_{12}$ polyhedron in the structure of antimonian dussertite. Thermal ellipsoids are drawn at the 50% probability level.

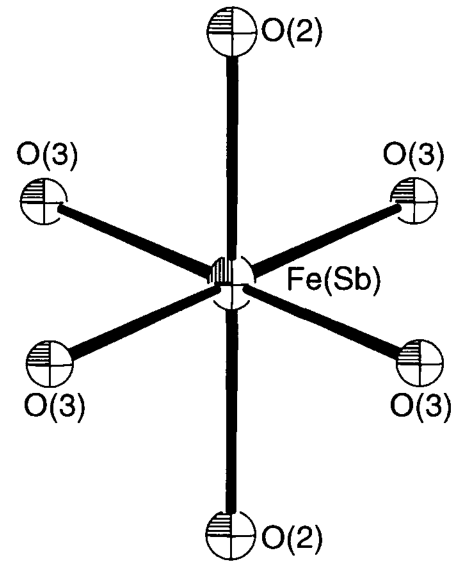

FIG. 2. The almost regular $(Fe,Sb)O_6$ octahedron. Thermal ellipsoids are drawn at the 50% probability level.

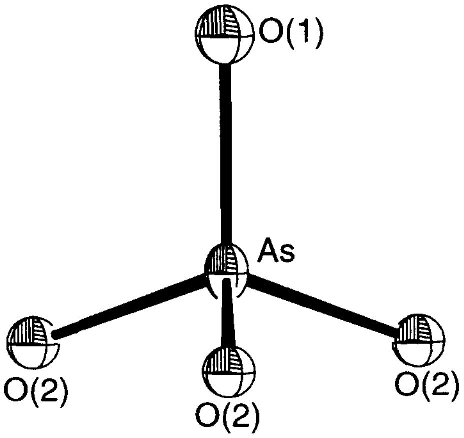

FIG. 3. The AsO_4 tetrahedron, showing the experimentally equivalent As-O bond lengths. Thermal ellipsoids are drawn at the 50% probability level.

The BVS value obtained for Ba, 2.46 *vu*, is unsatisfactory. However, it is known that Ba compounds in general tend to give poor BVSs (Brown and Wu, 1976). Ba is coordinated to six O(2) and six O(3) (with similar bond lengths, 2.863(5) and 2.885(6) Å) to form an unusually regular, ball-shaped icosahedron (Fig. 1). Therefore, a minor change in the Ba-O distance would influence the BVS to a large extent. The very minor Sr content of the crystal would be expected to result in only a very small decrease of the BVS. The average Ba-O bond lengths are slightly larger than the range of 2.834–2.860 Å determined for the Ba-Al-phosphate member of the crandallite group, gorceixite (Radoslovich, 1982) but smaller than the average Ba-O bond length in jagowerite, $BaAl_2(PO_4)_2(OH)_2$, (2.965 Å; Meagher *et al.*, 1974) or in baryte (2.95 Å, range 2.76–3.30 Å; Hill, 1977, Baur, 1981). No comparable data are available for arsenogorceixite, the other Ba arsenate end-member of the crandallite group.

In contrast to the disorder of the Ca site observed and suggested for crandallite and woodhouseite, respectively (Kato and Radoslovich, 1968; Blount, 1974; Kato, 1977), no disorder, or anomalously large displacement factors, for the Ba site were observed for dussertite (cf. Table 2). This is not unexpected because Ba, being larger than Ca, would more easily fit into the *A* cation 'cage'. The situation in dussertite is also quite different from that in Pb members of the crandallite and beudantite groups, all of which exhibit highly variable Pb-O bond lengths and displacement and disordering phenomena due to the influence of the lone electron pair of Pb^{2+}.

As pointed out above, both the refinement and the electron microprobe analyses clearly indicate that Sb partly occupies the Fe site but not the As site. The Fe/Sb ratio in the formula suggested by the refinement, $Ba(Fe^{3+}_{0.84},Sb^{5+}_{0.16})_3(AsO_4)_2(OH,H_2O)_6$, is in good agreement with the result from the electron microprobe analysis. Previously, Sb detected in crandallite- and beudantite-group minerals has been assumed to substitute for As (e.g. Smith *et al.*, 1953; Martin *et al.*, 1994). The disordered character of the Sb-Fe substitution can be compared to the situation in a Pb-sulphate member of the alunite group, osarizawaite, in which the *B* site in the structure is occupied by disordered Al^{3+}, Fe^{3+} and Cu^{2+} (Giuseppetti and Tadini, 1980).

The valency of Sb was assumed to be 5+ because dussertite crystallised in an oxidising environment and because of the strong prevalence of pentavalent Sb in comparable secondary Sb minerals (see more detailed discussion below). The nominal ionic radius of $^{[VI]}Fe^{3+}$, 0.645 Å, is similar to that of $^{[VI]}Sb^{5+}$, 0.60 Å (Shannon, 1976), whereas the radius of $^{[VI]}Sb^{3+}$ is 0.76 Å. The Sb^{5+} ion would not be accommodated easily into the four-coordinate As^{5+} site as the radius of $^{[IV]}As^{5+}$ is only 0.335 Å. The average coordination number of Sb^{5+} in inorganic compounds is 6.05, and those of Fe^{3+} and As^{5+} are 5.69 and 4.41, respectively (Brown, 1988). These data provide further support that Sb^{5+} enters the six-coordinate Fe^{3+} site in preference to the four-coordinate As^{5+} site.

The $(Fe,Sb)O_6$ octahedron is only slightly distorted (Fig. 2), and its symmetry and average (Fe,Sb)-O bond length, 2.004(1) Å, are similar to those of the FeO_6 octahedra in kintoreite (2.011 Å, Kharisun *et al.*, 1997) and plumbojarosite (2.008 Å, Szymański, 1985), whereas in aluminian beudantite, as expected, this value is slightly lower (1.997 Å, Szymański, 1988). Bond-valence calculations for the (Fe,Sb)-site in dussertite were conducted assuming 100 % occupancy of this site by each of the cations. For Fe^{3+} a value of 3.05 *vu* was calculated, and the result for Sb^{5+} was 5.01 *vu*. The BVS given in Table 4, 3.36 *vu*, was taken to be the weighted mean of those values on the basis of the refined composition, and reflects the increased average valency. The value for Sb^{5+}, 5.01 *vu*, is in very good agreement with the proposed Sb valency, and suggests that Fe-Sb substitution may be extensive.

The charge imbalance induced by the substitution of Sb^{5+} for Fe^{3+} amounts to 0.96 additional positive charges, which can be accounted for in two ways: firstly, a small percentage of the (ideally) four hydroxyls surrounding the (Fe,Sb) site may lose their hydrogens and so increase the net negative charge of the anions in the $(Fe,Sb)(OH)_4O_2$ octahedron; secondly, there might be vacancies on the (Fe,Sb) site. The total (Fe+Sb) content obtained by the microprobe analysis corresponds to 8.6 positive charges (neglecting the very minor amounts of Al) and could suggest the presence of vacancies. However, the estimated accuracy of the chemical analysis does not allow a definite conclusion to be drawn. No residual negative electron densities on the (Fe,Sb) site and the small anisotropic displacement factors indicate that this site is fully occupied. The modelled hydrogen-bonding network, and especially the unusually regular BaO_{12}, AsO_4 and $(Fe,Sb)O_6$ polyhedra, support the first assumption, i.e. that fewer hydroxyls are present in antimonian dussertite than might be expected for dussertite itself.

The role of antimony in other minerals

Other minerals in which Sb^{5+} shares the same site with Fe^{3+} include örebroite, $Mn_3^{2+}(Sb^{5+},Fe^{3+})Si(O,OH)_7$, bismutostibiconite, $Bi(Sb^{5+},Fe^{3+})_2O_7$, and melanostibite, $Mn(Sb^{5+},Fe^{3+})O_3$ (all formulae here and hereafter according to Fleischer and Mandarino, 1995, 1997). In the above three compounds, Sb exceeds Fe, unlike the situation in antimonian dussertite. Apparent ordering of Sb^{5+} and Fe^{3+} over their octahedrally coordinated sites is known only from the mineral filipstadite, $(Mn^{2+},Mg)_4Sb^{5+}Fe^{3+}O_8$ (Dunn *et al.*, 1988). On the other hand, Sb^{3+} and Fe^{3+} do not seem to substitute for each other, as indicated by the minerals chapmanite $Sb^{3+}Fe_2^{3+}(SiO_4)_2(OH)$ and derbylite, $(Fe^{3+},Fe^{2+},Ti)_7Sb^{3+}O_{13}(OH)$.

To our knowledge, trivalent Sb in secondary minerals formed by supergene processes, in strongly oxidising environments, has not been described yet. Examples of secondary minerals containing pentavalent Sb include camerolaite, $Cu_4^{2+}Al_2(HSb^{5+}O_4,SO_4)(CO_3)(OH)_{10}\cdot 2H_2O$, cualstibite, $Cu_6^{2+}Al_2Sb_3^{5+}O_{18}\cdot 16H_2O$, mammothite, $Pb_6Cu_4^{2+}AlSb^{5+}(SO_4)_2Cl_4O_2(OH)_{16}$, brizziite, $NaSb^{5+}O_3$, and bottinoite, $NiSb^{5+}(OH)_{12}\cdot 6H_2O$.

In minerals containing both Sb^{5+} and As^{5+}, such as richelsdorfite, $Ca_2Cu_5^{2+}Sb^{5+}[Cl(OH)_6(AsO_4)_4]\cdot 6H_2O$ (Süsse and Tillmann, 1987) and $Pb_3Sb^{5+}(OH)_6(SO_4)(AsO_4)\cdot 3H_2O$ (the Sb-dominant analogue of fleischerite; Sima *et al.*, 1996; Mandarino and Grice, 1997), these cations occupy different sites. There seem to be only two examples of supergene minerals in which Sb^{5+} possibly substitutes for As^{5+}: sabelliite, $(Cu,Zn)_2Zn[(As^{5+},Sb^{5+})O_4](OH)_3$ (Olmi *et al.*, 1995) and theisite, $Cu_5^{2+}Zn_5[(OH)_7|(As^{5+},Sb^{5+})O_4]_2$. The structure of theisite has not been determined and thus the proposed structural formula may not be correct. In the structure of sabelliite, whose refinement presented some inconsistencies (Olmi *et al.*, 1995), there are three As sites, one of which is reported to be partially occupied by disordered Sb and As and surrounded by four O atoms, forming a trigonal pyramid.

In dusssertite, the As atom forms a highly regular AsO_4 tetrahedron (Fig. 3) and the average As-O bond length, 1.684(3) Å, is almost identical to the values reported for the average arsenate tetrahedron in arsenates (1.683 Å, Shannon and Calvo, 1973; 1.682 Å, Baur; 1981). If As^{5+} had been replaced by the much larger Sb^{5+}, then an appreciably increased bond length would have been observed, probably accompanied by a distortion of the tetrahedron.

The As-O(1) bond is not shorter than the three As-O(2) bonds and indicates that O(1) is not protonated. This contrasts with the analogous bonds in most other members of the alunite family. In them, half of O(1) of the *X*-O(1) bond pair is reported to be a hydroxyl, with the *X*-O(1) bond therefore being shorter. The 'missing' hydrogen in dussertite is consistent with the proposed charge balance for the Sb-Fe substitution.

The unit cell volume, V = 831.3(3) Å^3, is slightly smaller than the value reported for an unanalysed but probably quite pure dussertite sample from the type locality (V = 835.1(1) Å^3, JCPDS-PDF 35-621). The lower values may reflect the very minor Sr and Al contents in the investigated crystal and/or the ionic radius of $^{[VI]}Sb^{5+}$ being slightly smaller than that of $^{[VI]}Fe^{3+}$ (0.60 *vs* 0.645 Å).

Suggestions for future work

The currently available data on crystal structures of the crandallite and beudantite and alunite groups demonstrate that it would be desirable to apply neutron diffraction methods to obtain more accurate data on the hydrogen positions and their influence on the symmetry. It may also prove useful to investigate the optical behaviour of biaxial members of the alunite family at different temperatures and search for possible phase transitions. Considering the potential use of crandallite-, beudantite- and alunite-group compounds as hosts for toxic heavy-metal waste, it would also be interesting to determine the maximum Sb solubility in Fe-members of these groups.

Acknowledgements

We thank Prof. E. Tillmanns, Vienna, for comments on the manuscript. This work was made possible by a Feodor-Lynen-Fellowship of the Alexander-von-Humboldt-Foundation, Bonn, Germany, to the first author. Part of the funds for this Fellowship were granted by the Australian Research Council (ARC) to Prof. T. J. White and Dr. A. Greeson (University of South Australia). The ARC is also thanked for support of the crystallographic facility.

References

Barth, T.F.W. and Berman, H. (1930) *Chem. Erde*, **5**, 22–42. [cited in Foshag (1937)].

Baur, W.H. (1981) Interatomic distance predictions for computer simulation of crystal structures. In *Structure and Bonding in Crystals* (M. O'Keeffe and A. Navrotsky, eds.), Vol. II, Academic Press, New York, 31–52.

Birch, W.D. and van der Heyden, A. (1997) Minerals of the Kintore and Block 14 open cuts at Broken Hill, New South Wales. *Austral. J. Mineral.*, **3**, 23–71.

Blanchard, F.N. (1989) New X-ray powder data for gorceixite, $BaAl_3(PO_4)_2(OH)_6{\cdot}H_2O$, an evaluation of d-spacings and intensities, pseudosymmetry and its influence on the figure of merit. *Powder Diffraction*, **4**, 227–30.

Blount, A.M. (1974) The crystal structure of crandallite. *Amer. Mineral.*, **59**, 41–7.

Brese, N.E. and M. O'Keeffe (1991) Bond-valence parameters for solids. *Acta Crystallogr.*, **B47**, 192–7.

Brown, I.D. (1988) What factors determine cation coordination numbers? *Acta Crystallogr.*, **B44**, 545–53.

Brown, I.D. and Altermatt, D. (1985) Bond valence parameters obtained from a systematic analysis of the inorganic crystal structure database. *Acta Crystallogr.*, **B41**, 241–7.

Brown, I.D. and Wu, K.K. (1976) Empirical parameters for calculating cation-oxygen bond valences. *Acta Crystallogr.*, **B32**, 1957–9.

Cowgill, U., Hutchinson, G.E. and Joensuu, O. (1963) An apparent triclinic dimorph of crandallite from a tropical swamp sediment in El Petén, Guatemala. *Amer. Mineral.*, **48**, 1144–53.

de Bruiyn, H., van der Westhuizen, W.A., Beukes, G.J. and Meyer, T.Q. (1990) Corkite from Aggeneys, Bushmanland, South Africa. *Mineral. Mag.*, **54**, 603–8.

de Meulenaer, J. and Tompa, H. (1965) The absorption correction in crystal structure analysis. *Acta Crystallogr.*, **19**, 1014–8.

Dunn, P.J., Peacor, D.R., Criddle, A.J. and Stanley, C.J. (1988) Filipstadite, a new Mn-Fe^{3+}-Sb derivative of spinel, from Långban, Sweden. *Amer. Mineral.*, **73**, 413–9.

Ferraris, G. and Ivaldi, G. (1984) *X*-OH and O-H···O bond lengths in protonated oxyanions. *Acta Crystallogr.*, **B40**, 1–6.

Fleischer, M. and Mandarino, J.A. (1995) *Glossary of Mineral Species 1995*. The Mineralogical Record

Inc., Tucson, USA.

Fleischer, M. and Mandarino, J.A. (1997) The first list of additions and corrections to the Glossary of Mineral Species 1995. *Mineral. Record*, **28**, 425–38.

Foshag, W.F. (1937) Carminite and associated minerals from Mapimi, Mexico. *Amer. Mineral.*, **22**, 479–84.

Giuseppetti, G. and Tadini, C. (1980) The crystal structure of osarizawaite. *Neues Jahrb. Mineral. Mh.*, 401–7.

Giuseppetti, G. and Tadini, C. (1987) Corkite $PbFe_3(SO_4)(PO_4)(OH)_6$, its crystal structure and ordered arrangement of tetrahedral cations. *Neues Jahrb. Mineral. Mh.*, 71–81.

Giuseppetti, G. and Tadini, C. (1989) Beudantite $PbFe_3(SO_4)(AsO_4)(OH)_6$, its crystal structure, tetrahedral site disordering and scattered Pb distribution. *Neues Jahrb. Mineral. Mh.*, 27–33.

Hill, R.J. (1977) A further refinement of the barite structure. *Canad. Mineral.*, **15**, 522–6.

Hintze, C. (1933) *Handbuch der Mineralogie*. Vol. I-4, Part 2, 721–41. Walter de Gruyter & Co., Berlin.

International Tables for X-ray Crystallography (1974) Vol. IV, Kynoch Press, Birmingham, England, 558 pp.

Jambor, J.L. and Dutrizac, J.E. (1983) Beaverite-plumbojarosite solid solutions. *Canad. Mineral.*, **21**, 101–13.

Jambor, J.L., Owens, D.R., Grice, J.D. and Feinglos, M.N. (1996) Gallobeudantite, $PbGa_3[(AsO_4),(SO_4)]_2(OH)_6$, a new mineral species from Tsumeb, Namibia, and associated new gallium analogues of the alunite-jarosite family. *Canad. Mineral.*, **34**, 1305–15.

Kato, T. (1977) Further refinement of the woodhouseite structure. *Neues Jahrb. Mineral. Mh.*, 54–8.

Kato, T. and Radoslovich, E.W. (1968) Crystal structures of soil phosphates. *Trans. 9th Int. Congr. of Soil Science, Vol. II, Int. Soc. of Soil Science, Adelaide, Australia*, 725–31.

Kharisun, Taylor, M.R., Bevan, D.J.M. and Pring, A. (1997) The crystal structure of kintoreite, $PbFe_3(PO_4)_2(OH,H_2O)_6$. *Mineral. Mag.*, **61**, 123–9.

Lengauer, C.L., Giester, G. and Irran, E. (1994) $KCr_3(SO_4)_2(OH)_6$: Synthesis, characterization, powder diffraction data, and structure refinement by the Rietveld technique and a compilation of alunite-type compounds. *Powder Diffraction*, **9**, 265–71.

Lottermoser, B.G. (1990) Rare-earth element mineralisation within the Mt. Weld carbonatite laterite, Western Australia. *Lithos*, **24**, 151–67.

Mandarino, J.A. and Grice, J.D. (1997) New minerals recently approved. *Mineral. Record*, **28**, 397–400.

Martin, M., Schlegel, F. and Siemroth, J. (1994) The mining district Niederschlag near Oberwiesenthal: Rare copper arsenates from the Saxonian Erzgebirge. *Lapis*, **19** (4), 13–22. (in German)

Meagher, E.P., Gibbons, C.S. and Trotter, J. (1974) The crystal structure of jagowerite: $BaAl_2P_2O_8(OH)_2$. *Amer. Mineral.*, **59**, 291–5.

Molecular Structure Corporation (1993) *teXsan – Single Crystal Structure Analysis Software, Version 1.6.* Molecular Structure Corporation, The Woodlands, TX 77381, USA.

O'Keeffe, M. (1991) *EUTAX, a Computer Program for Calculating Bond Valences*. Dept. of Chemistry, University of Arizona, USA.

Olmi, F., Sabelli, C. and Trosti-Ferroni, R. (1995) The crystal structure of sabelliite. *Eur. J. Mineral.*, **7**, 1331–7.

Palache, C., Berman, C. and Frondel, C. (1951) *Dana's System of Mineralogy*. 7th ed., Vol. II. John Wiley, New York.

Radoslovich, E.W. (1982) Refinement of the gorceixite structure in Cm. *Neues Jahrb. Mineral. Mh.*, 446–64.

Radoslovich, E.W. and Slade, P.G. (1980) Pseudo-trigonal symmetry and the structure of gorceixite. *Neues Jahrb. Mineral. Mh.*, 157–70.

Rattray, K.J., Taylor, M.R., Bevan, D.J.M. and Pring, A. (1996) Compositional segregation and solid solution in the lead dominant alunite-type minerals from Broken Hill, N.S.W. *Mineral. Mag.*, **60**, 779–85.

Schwab, R.G., Herold, H., Götz, C. and de Oliveira, N.P. (1990) Compounds of the crandallite type: Synthesis and properties of pure goyazite, gorceixite and plumbogummite. *Neues Jahrb. Mineral. Mh.*, 113–26.

Scott, K.M. (1987) Solid solution in, and classification of, gossan-derived members of the alunite-jarosite family, northwest Queensland, Australia. *Amer. Mineral.*, **72**, 178–87.

Shannon, R.D. (1976) Revised effective ionic radii and systematic studies of interatomic distances in halides and chalcogenides. *Acta Crystallogr.*, **A32**, 751–67.

Shannon, R.D. and Calvo, C. (1973) Refinement of the crystal structure of low temperature Li_3VO_4 and analysis of mean bond lengths in phosphates, arsenates, and vanadates. *J. Solid State Chem.*, **6**, 538–49.

Sima, I., Ettinger, K., Koppelhuber-Bitschnau, B., Taucher, J. and Walter, F. (1996) $Pb_3Sb(OH)_6(AsO_4,SO_4)_2 \cdot 3H_2O$, a new mineral isotypic with fleischerite. *Mitt. Österr. Mineral. Ges.*, **141**, 224–5. (in German)

Smith, R.L., Simons, F.S. and Vlisidis, A.C. (1953) Hidalgoite, a new mineral. *Amer. Mineral.*, **38**, 1218–24.

Süsse, P. and Tillmann, B. (1987) The crystal structure of the new mineral richelsdorfite, $Ca_2Cu_5Sb(Cl/(OH)_6/(AsO_4)_4) \cdot 6H_2O$. *Z. Kristallogr.*, **179**, 323–34.

Szymański, J.T. (1985) The crystal structure of plumbojarosite, $Pb[Fe_3(SO_4)_2(OH)_6]_2$. *Canad.*

Mineral., **23**, 659–68.

Szymański, J.T. (1988) The crystal structure of beudantite $Pb(Fe,Al)_3[(As,S)O_4]_2(OH)_6$. *Canad. Mineral.*, **26**, 923–32.

Walenta, K. (1966) Contributions to the knowledge of rare arsenate minerals with special respect to occurrences in the Black Forest. *Tschermaks Mineral. Petrogr. Mitt.*, **11**, 121–64. (in German)

Wise, W.S. (1975) Solid solution between the alunite, woodhouseite, and crandallite mineral series. *Neues Jahrb. Mineral. Mh.*, 540–5.

[*Manuscript received 1 May 1998:*
revised 1 July 1998]